High spatial correspondence at a columnar level between activation and resting state fMRI signals and local field potentials

Zhaoyue Shi[a,b,1], Ruiqi Wu[b,c], Pai-Feng Yang[b,c], Feng Wang[b,c], Tung-Lin Wu[a,b], Arabinda Mishra[b,c], Li Min Chen[b,c], and John C. Gore[a,b,c,d]

[a]Department of Biomedical Engineering, Vanderbilt University, Nashville, TN 37235; [b]Vanderbilt University Institute of Imaging Science, Vanderbilt University, Nashville, TN 37235; [c]Department of Radiology and Radiological Sciences, Vanderbilt University, Nashville, TN 37232; and [d]Department of Physics and Astronomy, Vanderbilt University, Nashville, TN 37232

Edited by Marcus E. Raichle, Washington University in St. Louis, St. Louis, MO, and approved April 3, 2017 (received for review December 14, 2016)

Although blood oxygenation level-dependent (BOLD) fMRI has been widely used to map brain responses to external stimuli and to delineate functional circuits at rest, the extent to which BOLD signals correlate spatially with underlying neuronal activity, the spatial relationships between stimulus-evoked BOLD activations and local correlations of BOLD signals in a resting state, and whether these spatial relationships vary across functionally distinct cortical areas are not known. To address these critical questions, we directly compared the spatial extents of stimulated activations and the local profiles of intervoxel resting state correlations for both high-resolution BOLD at 9.4 T and local field potentials (LFPs), using 98-channel microelectrode arrays, in functionally distinct primary somatosensory areas 3b and 1 in nonhuman primates. Anatomic images of LFP and BOLD were coregistered within 0.10 mm accuracy. We found that the point spread functions (PSFs) of BOLD and LFP responses were comparable in the stimulus condition, and both estimates of activations were slightly more spatially constrained than local correlations at rest. The magnitudes of stimulus responses in area 3b were stronger than those in area 1 and extended in a medial to lateral direction. In addition, the reproducibility and stability of stimulus-evoked activation locations within and across both modalities were robust. Our work suggests that the intrinsic resolution of BOLD is not a limiting feature in practice and approaches the intrinsic precision achievable by multielectrode electrophysiology.

BOLD fMRI | local field potential | point spread function | resting state correlations | primary somatosensory cortex

Functional MRI (fMRI) is well established as a neuroimaging technique for detecting and delineating regions in the brain that change their levels of activity in response to specific experimental conditions (1–3). In addition, the discovery and analysis of synchronized fluctuations of low-frequency MRI signals between different brain regions at rest have provided a powerful approach to probe functional connectivity between regions and to delineate functional circuits (4–7). However, stimulus-evoked fMRI responses usually rely on detecting blood oxygenation level-dependent (BOLD) signal changes, which reflect hemodynamic processes, and thus are indirect indicators of neuronal activity. The measured extents of BOLD activations depend on the integrated contributions from the intrinsic spatial distributions of the neural activity involved, the effects of converting neural electrical activity to spatial distributions of metabolic and hemodynamic changes that then affect MRI signals, and the effects of image acquisitions and reconstruction with limited resolution, but the relative contributions of these to detected signals remain obscure. Precise interpretations of fMRI studies require a better understanding of the quantitative relationships between BOLD signal changes and their corresponding electrophysiological signatures. Several previous studies have focused on understanding what types of electrophysiological signals [e.g., spike vs. local field potential (LFP)] drive (or correlate) with fMRI signals (8–11) and have confirmed that fMRI signals are reliable indicators of associated neuronal activity (12, 13). Few studies, however, have examined the relationships between fluctuations of fMRI signals and spontaneous electrophysiological signal variations at rest (14, 15). No study, to our knowledge, has directly compared the spatial distributions of BOLD and LFP signals in both information processing (to external stimuli) and their correlation profiles in a resting state. The ultimate spatial resolution and functional specificity of connectivity metrics depend on the local spread of BOLD signals beyond those of underlying neural activity, especially at the mesoscopic level of functional specialization. Here we report the use of high-resolution fMRI at high field strength (9.4 T) to measure the spatial extents of BOLD activations in response to stimuli with high spatial specificity, as well as the spatial profiles of single-voxel local correlations in a resting state, in the primary somatosensory cortex of nonhuman primates. We then compare these with the extents of LFPs, and their interelectrode correlations, in the same conditions and the same brain region. Our results shed light on the intrinsic limits of BOLD fMRI at high field and the relationship of BOLD signal changes to underlying electrophysiological activity.

In the experiments described, we directly compared the spatial extents or point spread functions (PSFs) of stimulated activations in response to minimal vibrotactile stimulation of single digits and the profiles of intervoxel resting state correlations of responding voxels. The locations and extents of activations and resting state correlation profiles for high-resolution BOLD at 9.4 T

Significance

We found that blood oxygenation level-dependent (BOLD) signal changes within single-digit representation columns in the primary somatosensory cortices of areas 3b and 1 aligned spatially very closely with local field potential (LFP) signals in response to tactile stimulation. Moreover, resting state BOLD fMRI and LFP signals also exhibited very similar intervoxel spatial correlation profiles. These findings indicate that at a columnar level, BOLD signals faithfully reflect underlying neuronal activity both during information processing and at rest. Importantly, the spread of BOLD activity and correlations at high field are no greater than the extent of LFP signals. These results demonstrate that high-field fMRI has the ability to delineate brain activity at the columnar level, and BOLD signals faithfully reflect electrophysiological activity.

Author contributions: L.M.C. and J.C.G. designed research; Z.S., R.W., P.-F.Y., F.W., and T.-L.W. performed research; Z.S., R.W., and A.M. contributed new reagents/analytic tools; Z.S. analyzed data; and Z.S., L.M.C., and J.C.G. wrote the paper.

The authors declare no conflict of interest.

This article is a PNAS Direct Submission.

[1]To whom correspondence should be addressed. Email: zhaoyue.shi@vanderbilt.edu.

This article contains supporting information online at www.pnas.org/lookup/suppl/doi:10.1073/pnas.1620520114/-/DCSupplemental.

and LFPs, using two 7 × 7 multichannel microelectrode arrays include the digit representation regions of two functionally distinct somatosensory subregions 3b and 1 in individual monkeys. We found that the mean full widths at half maximum (FWHMs) of the fitted PSFs of BOLD and LFP responses to tactile stimulation in both areas 3b and 1 for stimulus-evoked conditions were around 1 mm, and the magnitudes of stimulus responses in area 3b were stronger than those in area 1 and extended in a medial to lateral direction. The intervoxel correlation profiles of resting state BOLD and spontaneous LFP signals for individual voxels or electrodes were slightly wider than those produced by stimulation. In addition, we found that the estimated widths of the PSFs of the BOLD responses were significantly smaller at resolution of 0.274 × 0.274 mm^2 than at lower resolution of 0.547 × 0.547 mm^2, indicating residual partial volume effects even at this scale. We found no differences in the widths of the PSFs between LFP and BOLD fMRI at a high resolution at 9.4 T in both stimulus and resting state conditions. BOLD fMRI signals obtained at submillimeter resolution at high field are thus reliable and accurate indicators of underlying neural activity in both stimulation and resting state conditions.

Results

Comparable Spatial Profiles of BOLD and LFP Responses to Tactile Stimulation in Areas 3b and 1. To compare spatial response profiles to external stimuli between fMRI and LFPs, we estimated the FWHMs along the major and minor axes and the area and ratio of axes for each BOLD activation and the corresponding LFP responses. Fig. 1 *A–D* shows examples of fMRI and LFP activation maps to D3 tactile stimulation in both areas 3b and 1 of the same subject. Fig. 1 *C* and *D* shows 3D plots of the overall activation patterns in areas 3b and 1 and their local spatial profiles. By comparing measurements across all studies, we found no significant differences between BOLD and LFP estimates of the FWHMs along major and minor axes (Fig. 1 *E* and *G*), areas (Fig. 1*F*), or major/minor axis ratio (Fig. 1*H*, comparing blue and green columns in Fig. 1 *E–H*) in both area 3b and area 1. For both BOLD and LFP responses, activation foci in area 3b have an elongated oval shape, with the major axis orientated in a lateral to medial direction that is along the line of digit tip-to-tip representations. In contrast, activation foci in area 1 are aligned in an anterior to posterior direction, along the line distinguishing digit bottom from top and orthogonal to the interareal border. For BOLD responses (n = 6 subjects), the FWHM of the major axis (1.08 ± 0.13 mm) of single-digit activation in area 3b was statistically significantly ($P < 0.001$, Wilcoxon signed-rank test) larger than that of the minor axis (0.71 ± 0.21 mm), whereas the FWHM of the major axis (0.95 ± 0.21 mm) in area 1 was not significantly different ($P > 0.05$) from that of the minor axis (0.81 ± 0.09 mm). For stimulus-evoked LFP responses (n = 4 subjects), the FWHM of the major axis (1.07 ± 0.16 mm) was statistically significantly ($P < 0.001$) larger than that of the minor axis (0.78 ± 0.20 mm) in area 3b; again, in area 1, the FWHM of the major axis (0.96 ± 0.12 mm) was not significantly different ($P > 0.05$) from that of the minor axis (0.84 ± 0.16 mm). Activation areas of area 3b (BOLD: 0.61 ± 0.23 mm^2; LFP: 0.69 ± 0.15 mm^2) and area 1 (BOLD: 0.61 ± 0.18 mm^2; LFP: 0.68 ± 0.23 mm^2) did not differ ($P > 0.05$). For both BOLD and LFP signals, Table 1 summarizes these results.

Comparable Local Voxel–Voxel Correlation Profiles of Resting State BOLD and LFP Signals. We next measured the FWHM, area, and major/minor axis ratio of intervoxel correlation profiles of resting state BOLD signals for foci of stimulus-evoked activations and compared these with corresponding resting state LFP signals. We selected single voxels that showed the strongest responses to tactile stimuli as seeds in areas 3b and 1 (Fig. 2). Within a single-digit representation in areas 3b and 1, the local intrinsic functional connectivity profiles of resting state BOLD and LFP signals are very similar. FWHMs of the major and minor axes of the resting state intervoxel BOLD correlation profiles were, respectively, 1.16 ± 0.15 mm and 0.83 ± 0.14 mm in area 3b and 1.07 ± 0.17 mm and 0.90 ± 0.08 mm in area 1. For resting state LFP signals, FWHMs of the major and minor axes of the resting state intervoxel LFP correlation profiles were 1.14 ± 0.20 mm and 0.89 ± 0.17 mm in area 3b and 1.11 ± 0.19 mm and 0.97 ± 0.16 mm in area 1. These LFP measures were not significantly different from resting state BOLD estimates.

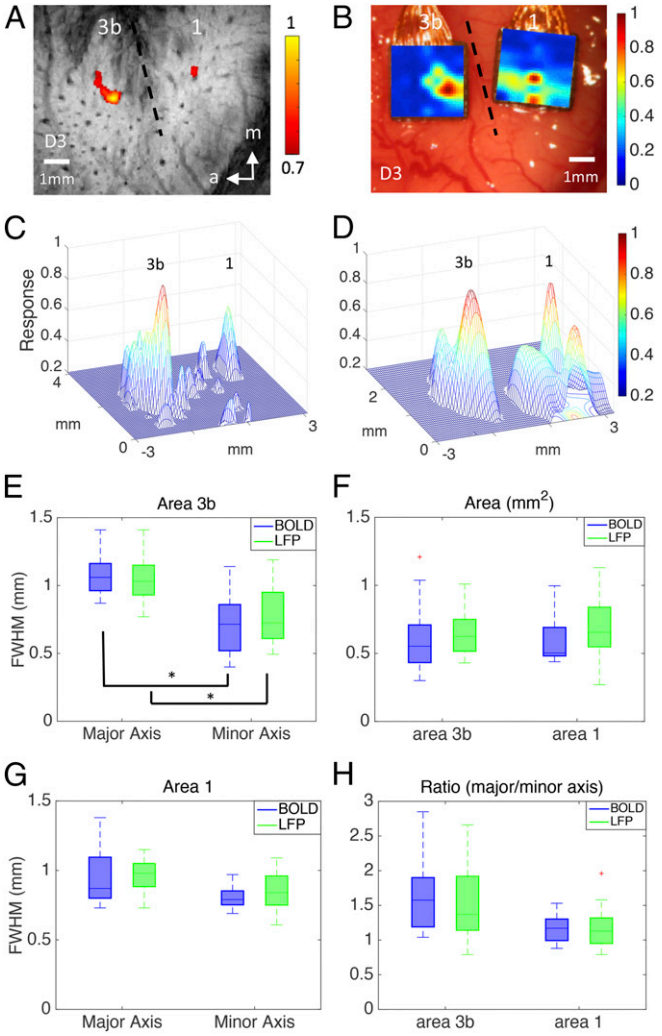

Fig. 1. Spatial extents of tactile stimulus-evoked BOLD and LFP activation in areas 3b and 1. One case is shown in *A–D*; entire population data are given in *E–H*. (*A*) BOLD activations in response to vibrotactile stimulation of digit 3 distal fingertip in areas 3b and 1. Activation map is thresholded at 0.7 of normalized percentage signal changes, with a peak value of 1. Dotted line represents estimated interareal border between areas 3b and 1. (*B*) Corresponding LFP activation map in response to identical stimulation used in fMRI experiment shown in *A*. (*C*) 3D illustration of the BOLD activation map shown in *A*. The *x* and *y* axes represent the location of the voxel in millimeters, whereas the *z* axis represents the normalized percentage of signal change between the prestimulus and stimulus periods. (*D*) 3D illustration of the LFP activation map shown in *C*. (*E*) FWHM of area 3b, significance at *$P <$ 0.001 (Wilcoxon signed-rank test). (*F*) The area values of 3b and 1. (*G*) FWHM of area 1. (*H*) The ratio of major and minor axis of 3b and 1. A total of 30 runs from six monkeys were acquired for BOLD measurements, and 30 runs from four monkeys were acquired for LFP measurements.

Table 1. FWHM from all subjects for stimulated and resting-state BOLD and LFP

	Stimulated*				Resting state*			
	Area 3b (mm)		Area 1 (mm)		Area 3b (mm)		Area 1 (mm)	
Modality	Major axis**	Minor axis**	Major axis	Minor axis	Major axis	Minor axis	Major axis	Minor axis
BOLD	1.08 ± 0.13	0.71 ± 0.21	0.95 ± 0.21	0.81 ± 0.09	1.16 ± 0.15	0.83 ± 0.14	1.07 ± 0.17	0.90 ± 0.08
LFP	1.07 ± 0.16	0.78 ± 0.20	0.96 ± 0.12	0.84 ± 0.16	1.14 ± 0.20	0.89 ± 0.17	1.11 ± 0.19	0.97 ± 0.16

*indicates significance ($P < 0.05$) between resting-state and stimulated conditions;
**indicates significance ($P < 0.001$) between major and minor axes of area 3b of both modalities in the stimulated condition.

Local Spatial Extents of Resting State Functional Connectivity Are Wider than Those of Cortical Responses to Stimuli for BOLD and LFP Signals. Direct comparisons of the FWHM measures between stimulation and resting states revealed that the PSF of resting state voxel–voxel correlations is significantly wider than that of stimulation responses ($P < 0.05$; Fig. 3), regardless of specific area examined (area 3b or area 1). For example, in both areas 3b and 1, the FWHM of the major axis (1.16 ± 0.15 mm and 1.07 ± 0.17 mm) and that of the minor axis (0.83 ± 0.14 mm and 0.90 ± 0.08 mm) of the resting state BOLD correlations were larger than both the major axis (1.08 ± 0.13 mm and 0.95 ± 0.21 mm) and minor axis (0.71 ± 0.21 mm and 0.81 ± 0.09 mm) in the stimulated BOLD activation maps. Moreover, in both areas 3b and 1, the FWHM of the major axis (1.14 ± 0.20 mm and 1.11 ± 0.19 mm) and that of the minor axis (0.89 ± 0.17 mm and 0.97 ± 0.16 mm) of the resting-state LFP electrode–electrode coherence were larger than both the major (1.07 ± 0.16 mm and 0.96 ± 0.12 mm) and minor (0.78 ± 0.20 mm and 0.84 ± 0.16 mm) axes in the stimulated LFP activation maps.

Reproducibility and Spatial Agreement Between Activation Locations Measured by BOLD and LFP. Last, we examined the reproducibility of the activation centers of area 3b and area 1 of stimulus-evoked BOLD and LFP across runs and the spatial relationships between

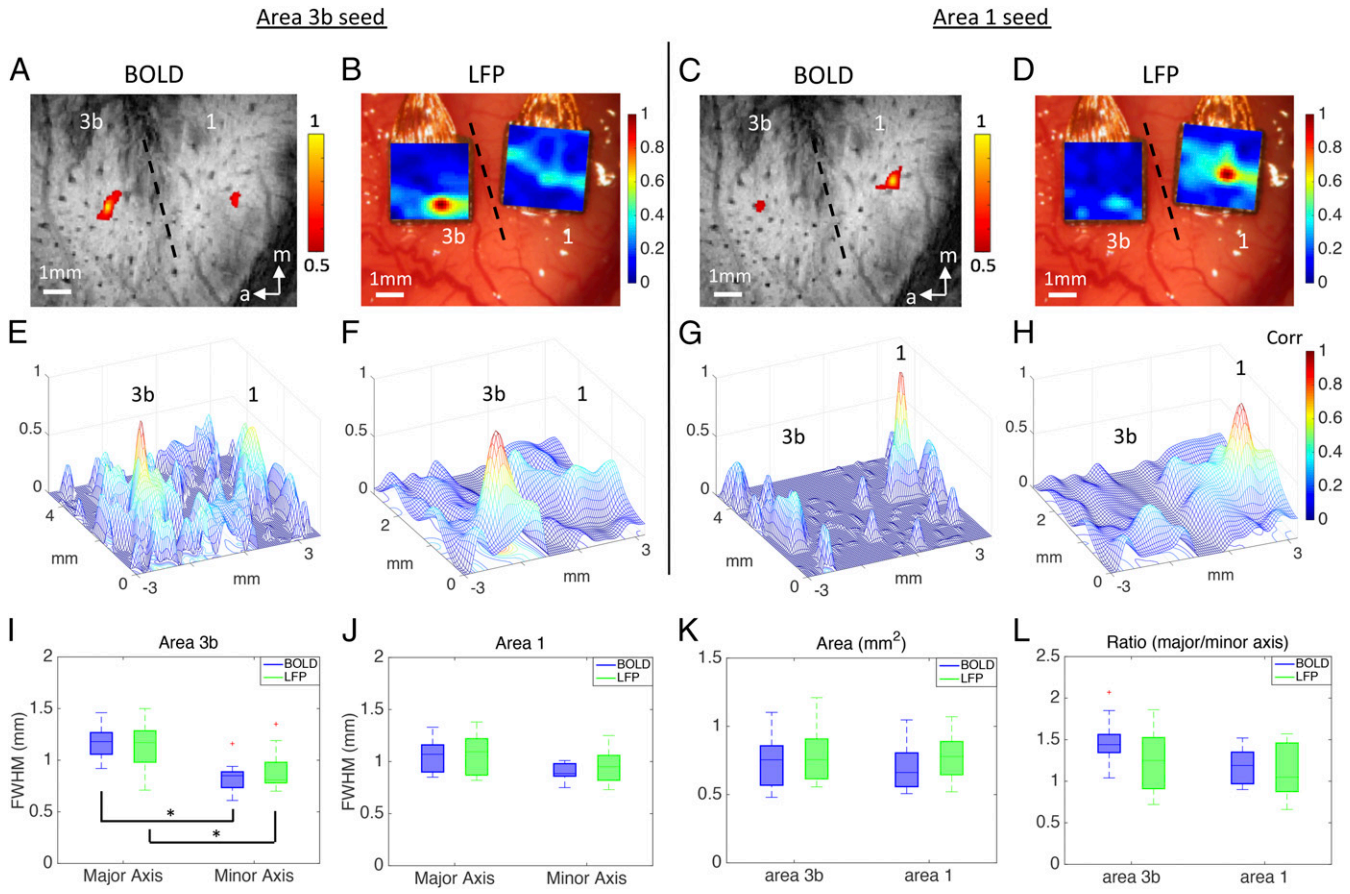

Fig. 2. Spatial extent of resting-state fMRI and LFP connectivity within areas 3b and 1. One case is shown in *A–H*, and the entire population data are given in *I–L*. (*A*) BOLD correlation map in the resting state condition. Seed voxel was placed in the digit region in area 3b for voxel-wise correlation analysis. Correlation map was thresholded at $r > 0.5$, with a peak of 1. Dotted line represents estimated interareal border between areas 3b and 1. (*B*) Corresponding LFP correlation map of seed area 3b in the resting-state condition. (*C*) BOLD correlation map of seed area 1. (*D*) Corresponding LFP correlation map of seed area 1. (*E–H*) 3D plots of correlation spatial profiles of BOLD and LFP in areas 3b and 1, with *x* and *y* axes representing the location of the voxel (mm), and *z* axis representing the correlation values. (*I*) FWHM of area 3b in the resting state condition, significance at $^*P < 0.001$. (*J*) FWHM of area 1. (*K*) The area values of 3b and 1 in the resting-state condition. (*L*) The major and minor axis ratio of 3b and 1 at rest. A total of 18 runs from six animals were acquired for BOLD measurements, and 22 runs from four monkeys were acquired for LFP measurements.

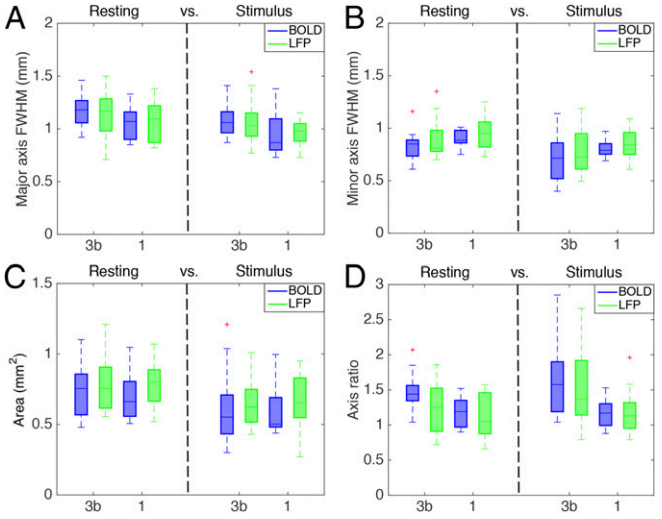

Fig. 3. Comparison of point-spread functions of BOLD and LFP signals in areas 3b and 1, between resting state and stimulation. (*A*) FWHM of major axis for areas 3b and 1. (*B*) FWHM of minor axis for both areas. (*C*) The area values of 3b and 1 in both resting and stimulus conditions. (*D*) The major and minor axis ratio of 3b and 1 in both conditions.

BOLD and LFP activation maps in each individual animal. Within each fMRI session, we determined the center of mass of each activation focus and then calculated the means and SDs of distances between corresponding centers on separate stimulus runs for all runs within each session and looked at the variation across study sessions and subjects ($n = 6$ animals, 30 runs). The intercenter distance variation for BOLD was 0.23 ± 0.05 mm for area 3b, and 0.24 ± 0.05 mm for area 1. The spatial variation of activation centers was thus close to the size of one voxel (in-plane resolution of 0.274×0.274 mm^2). For stimulus-evoked LFP activation maps ($n = 4$ animals, 30 runs), the intercenter distance was 0.10 ± 0.03 mm for area 3b and 0.12 ± 0.04 mm for area 1, respectively. The intercenter distance was smaller than the spatial spacing (0.4 mm) between two adjacent electrodes. Direct comparisons between BOLD and LFP maps revealed that the intercenter distance variation between modalities was 0.32 ± 0.06 mm for area 3b and 0.35 ± 0.09 mm for area 1. The spatial agreement was close to the range of a single BOLD (0.274×0.274 mm^2) and LFP (0.40×0.40 mm^2) mapping voxel. Anatomic images of both modalities were coregistered within 0.10 mm accuracy.

Discussion

This study aimed to determine to what extent the local spatial profile of BOLD fMRI signals corresponds to underlying neuronal activity at a submillimeter, cortical modular scale. We compared the spatial extents (FWHMs of major and minor axes, area, and major/minor axis ratio) and activation center locations of BOLD signal changes with those of 'gold standard' electrophysiological LFP measurements during tactile stimulation, and the local correlation profiles in a resting state, in the primary somatosensory cortex of New World monkeys. Using 0.274×0.274 mm^2 in-plane resolution BOLD fMRI at 9.4 T and LFP recordings with 98-channel (two 7×7) microelectrode arrays (0.40×0.40 mm^2 in spacing), we compared BOLD and LFP measures in four cases: stimulus-evoked BOLD versus LFP responses, resting state BOLD versus spontaneous LFP signal changes, stimulus-evoked versus resting-state maps in each modality, and areas 3b versus 1. We found that the FWHM of PSFs of BOLD and LFP responses to tactile stimuli were comparable and around 1 mm, which is the size of one single digit representation. Both modalities captured elongated stimulus responses in the lateral to medial direction in area 3b, a feature that was absent in area 1. In addition, the PSFs of intervoxel local correlation profiles of both resting state BOLD and LFP signals were slightly, but significantly, wider ($P < 0.05$) than those of stimulus activations. The elongated spatial profiles of digit representations in area 3b were also present in resting state correlations. Moreover, variation in activation centers for repeated measurements by BOLD was less than 0.25 mm and was smaller for LFPs, whereas the separation of activation centers between modalities was very similar, indicating the stability and reproducibility of stimulus activation locations within and across two modalities. Extending previous observations of the closely correlated signal increases of LFP and BOLD signals to stimuli (9, 12), here we provide further evidence of a close and strong spatial correspondence between BOLD and LFP signals in response to stimulation and in a resting state. The strong agreement between BOLD and LFP in stimulation and resting states indicates that local extents of activation and correlation profiles of resting state BOLD signals are constrained by neuronal properties, and not other factors. BOLD fMRI at high field and at submillimeter resolution directly and faithfully reflects the spatial distribution of underlying neural activity.

Implications for High-Resolution BOLD fMRI at High Field. The PSF of BOLD mapping signals sets the theoretical limits of spatial specificity and resolution of functional imaging. The width of the measured BOLD PSF is a convolution of the contributions from the intrinsic spatial distribution of the neural activity involved, the effects of converting neural electrical activity to a spatial distribution of metabolic and hemodynamic changes that affect MRI signals, and the effects of image acquisition and reconstruction with finite resolution. The PSF that we report in S1 cortex is narrower than those reported previously [3.5 mm at 1.5 T (16), 3.9 mm at 3 T (17), and 2 mm at 7 T (18)]. We attribute this difference to the effects of magnetic field on the functional mapping signals used and to our use of relatively high-resolution acquisitions. The BOLD response at lower magnetic fields (e.g., 1.5 T) may be dominated by signals from larger draining veins with little contribution from microvasculature. At high fields, the relative contributions of both intravascular signals and the effects of larger vessels on extravascular dephasing to the overall fMRI signal changes are substantially diminished (19, 20). The increase in the intrinsic width of the PSF of BOLD signals at 1.5 T and 3 T may be attributed to the presence of greater large vessel contributions to signal dephasing of the extravascular water at those lower fields (21, 22). Moreover, it is likely that measurements acquired at lower field and resolution also reflected the intrinsic resolution limitations of the image acquisitions. The higher resolution that we used made it possible to reduce partial-volume effects and more closely approach the intrinsic limits of BOLD. Functional images acquired with an in-plane resolution of 0.547×0.547 mm^2 yielded PSFs significantly wider than those obtained from higher-resolution functional images with an in-plane resolution of 0.274×0.274 mm^2, indicating that partial volume averaging may broaden regions of activation even at this scale, and confirming that higher-resolution functional images increase the spatial specificity of BOLD fMRI so that the intrinsic BOLD PSF need not be a limiting feature in practice. This suggests that the spatial specificity of submillimeter resolution BOLD fMRI at high magnetic field provides a reliable tool for the investigation of cortical micro-organization.

Spatial Extents of BOLD and LFP Signals in S1 Cortex. In this study, we pushed the fMRI spatial resolution to submillimeter (0.274×0.274 mm^2) and compared it directly with LFP recordings from the same region with a resolution of 0.40×0.40 mm^2. We found that the FWHMs of BOLD activations at 9.4 T were around 1 mm, which is four times the acquired voxel size. We found

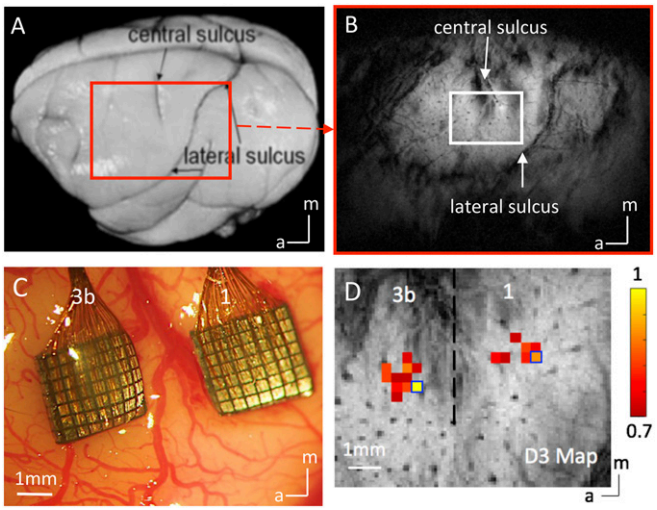

Fig. 4. Experimental set up for mapping areas 3b and 1 of S1 cortex with submillimeter-resolution fMRI and 98 channel Utah array. (*A*) Major landmarks used to identify digit regions in areas 3b and 1 of S1 are visible on the postmortem squirrel monkey brain. The red box indicates the imaging field of view. (*B*) In an oblique coronal image acquired with T2* weighting, sulci and surface and transcortical vessels appear as dark lines and dots. (*C*) Blood vessel map shows the two 7 × 7 multichannel electrode arrays were inserted in the digit regions of areas 3b and 1 under surgical microscope in one representative monkey. (*D*) Corresponding BOLD fMRI activation map to vibrotactile stimulation of the D3 distal finger pad in areas 3b and 1 of S1 cortex. Normalized percentage signal change maps were thresholded at 0.7. Dotted black line indicates the approximate border between areas 3b and 1. Blue boxes show the selected seed voxels used in resting state functional connectivity analysis. (Scale bar, 1 mm.) a, anterior; m, medial.

excellent spatial agreement between stimulus-evoked BOLD and LFP responses in both area 3b and area 1.

Despite their widespread adoption as measures of functional connectivity, little is known as to how the low-frequency temporal fluctuations of resting state BOLD signals vary locally, and whether correlated fluctuations actually reflect synchronized spontaneous LFP signal variations at rest. Our previous studies in monkeys demonstrated that the strength of resting state BOLD signal correlations between brain regions was related closely to the strength of anatomic connections and whether those areas coactivated to the same stimuli (23). These observations suggest that neurons that share similar functions and anatomically dense connections exhibit highly synchronized signal fluctuations at rest. A residual question is whether the extent of the activity of functionally homogeneous neurons is accurately reflected by resting state fMRI correlations. In this study, we assessed the spatial relationship between resting state BOLD and LFP measurements and between stimulus response and local correlation profiles in a well-described cortical modular structure, the single-digit representations in areas 3b and 1 in monkeys. Our data demonstrate that the spatial extents of high correlations of both BOLD and LFP signals are constrained tightly to the anatomic boundaries of neurons receiving inputs from the same digit region-tips in a similar manner. The different PSF shapes identified in area 3b versus area 1 (elongated vs. round) further support the correspondence between neural electrical signals and BOLD signal fluctuation at rest at the submillimeter to millimeter scale. The high degree of agreement between PSFs of BOLD and LFP signals in both stimulation and resting states supports the notion that synchrony within a functionally homogeneous population of neurons determines the strength of local resting state correlation measures in either modality. The close coupling between columnar structures and local microvasculature likely also contributed to the high spatial agreement between two modalities (24). The tactile stimulus we used is subtle and activates only a small (~1 mm) piece of cortex compared with much broader activation previously reported in the visual cortex (25). It is very likely the 8-Hz digit stimuli activate only a fraction of each digit column, as this stimulus drives predominantly slow-adapting neurons (26, 27). If the spontaneous fluctuations in the resting state are driven by common inputs [e.g., from thalamus or cortical–cortical connections (28)], then the wider FWHMs for correlation profiles could reflect that more neurons were engaged by these common inputs. What these inputs are and to what extent the differences in common input are reflected in the resting state functional connectivity signals are of great interest for further investigation. Together with our recent findings of the close relationship between interregional BOLD and LFP correlations (29), the tight local spatial relationship between BOLD and LFP signals shows that resting state BOLD signals are reflective of underlying neuronal electrical activity, and therefore, can be used to probe functional connectivity.

The Primary Somatosensory Cortex of New World Monkeys. Studies of nonhuman primates provide a crucial linkage between a large existing literature of animal data obtained with invasive methods and human fMRI data involving higher mental functions. We studied the digit representation regions in primary somatosensory areas 3b and 1 of monkeys at 9.4 T. This preparation is a unique experimental model for studies of brain activation and connectivity, with several advantages. First, single-digit representation is an example of classical modular functional structures, which are the basic information processing units of neocortex. Second, the anatomic connections and receptive field properties of neurons in the digit regions areas 3b and 1 have been intensively mapped with functional imaging, electrophysiological, and anatomic methods

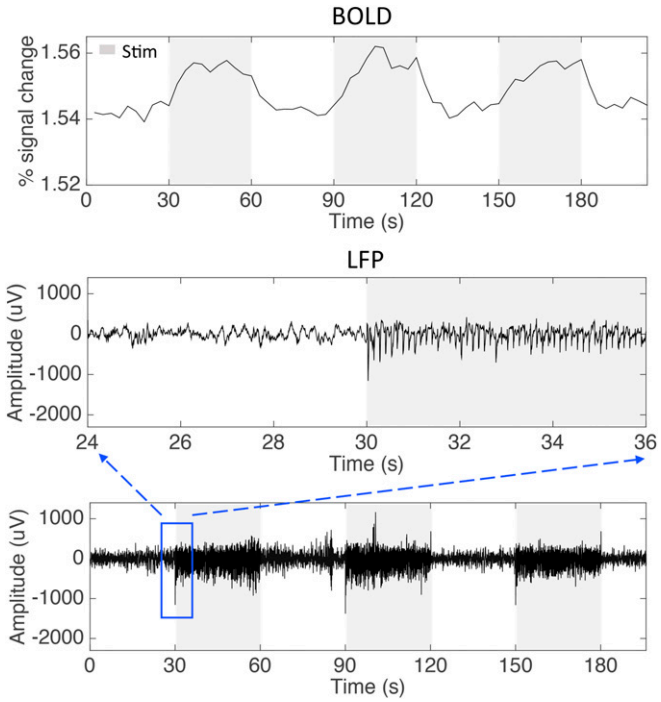

Fig. 5. Representative BOLD and LFP signal changes to vibrotactile stimuli. (*A*) Time series of BOLD signal changes to 8 Hz vibrotactile stimuli of single digit extracted from area 3b voxel. (*B*) Recordings of raw broadband LFP in response to the identical tactile stimulation as applied in BOLD mapping experiment shown in *A*. Blue box shows the sampling window.

NEUROSCIENCE

(23, 30, 31). Third, our previous studies have established qualitative spatial relationships between BOLD responses to tactile stimuli and neuronal responses (assessed through spiking activities) and underlying intrinsic horizontal connections (32).

Methods

Animal Preparation. Six squirrel monkeys (*Saimiri bolivians*) were included in this study, and all underwent fMRI scans. Four of the six monkeys underwent 98-channel microelectrode array recording sessions. Detailed procedures have been described in previous publications (33) and *SI Text*. All procedures were in compliance with and approved by the Institutional Animal Care and Use Committee of Vanderbilt University and followed the guidelines of the National Institutes of Health *Guide for the Care and Use of Laboratory Animals* (34).

fMRI Data Acquisition and Analysis. MRI was performed with a 9.4-T, 21-cm bore Varian Inova magnet (*SI Text*). Scout images obtained using a fast gradient-echo sequence were used to define a volume covering the primary somatosensory cortex (Fig. 4 *A* and *B*). For stimulation runs, we computed activation maps based on the percentage of BOLD signal change between prestimuli periods (seven of ten imaging volumes before stimulus onset) and stimuli presentation periods (Fig. 5*A*).

LFPs Recording and Analysis. Guided by MRI maps and blood vasculature pattern, two 7×7 multichannel Utah electrode arrays (Fig. 4*C*; 98 channels in total, spacing between each electrode, 400 μm) were carefully inserted into area 3b and area 1 cortex (*SI Text*). LFP signals were sampled at 500 Hz and then band-pass filtered between 1 and 150 Hz for quantification. Fig. 5*B* shows an example of LFP broadband (1–150 Hz) raw data, including 30 s of prestimulus period and 30 s of stimulus presentation.

Measurements of the PSF of BOLD fMRI Signals in Stimulation and Resting State. We identified activation foci in areas 3b and 1 whose shapes could be well approximated as elliptical (*SI Text*). The spatial distributions of percentage of BOLD signal changes along the major and minor axes were then fit with Gaussian functions. For resting state fMRI runs, region of interest (ROI) seeds were identified on the basis of the stimulus-evoked activation maps. The voxels with the highest percentage BOLD signal change were chosen as the seeds for each digit in either area 3b or area 1 (Fig. 4*D*). Correlation coefficients were computed for each voxel surrounding the seed. Identical spatial fitting procedures were applied to derive the FWHM, area, and major/minor axis ratio of Gaussian PSFs of fitted local correlation profiles. The same spatial ellipsoid fitting method was used to quantify the PSFs of LFP signals.

Comparison of Locations of BOLD Versus LFP Activations. Coregistrations of fMRI activation maps with LFP activation maps were accomplished using anatomic landmarks, surface blood vessel patterns, and a point-based coregistration algorithm. Forty to 80 pairs of reference points were used as landmarks in the 2D geometric nonlinear transformation. Apparent black dots on the T_2* MR structural images were caused by transcortical vessels. Their corresponding landmarks were visible on the LFP blood vessel maps as well. After coregistration, the point-to-point spatial offsets (square distances) of the predefined 40–80 reference pairs were computed as coregistration accuracy. For both BOLD and LFP foci, the stabilities of the activation centers were quantified by the spatial shifts (distance) between the centers from all stimulus runs within each session (*SI Text*).

ACKNOWLEDGMENTS. The authors gratefully acknowledge Fuxue Xin and George H. Wilson, III, for their assistance with data collection and Chaohui Tang for animal preparation. This work was supported by NIH Grants NS078680 (to J.C.G.) and NS069909 (to L.M.C.).

1. Ogawa S, Lee TM, Kay AR, Tank DW (1990) Brain magnetic resonance imaging with contrast dependent on blood oxygenation. *Proc Natl Acad Sci USA* 87:9868–9872.
2. Bandettini PA, Wong EC, Hinks RS, Tikofsky RS, Hyde JS (1992) Time course EPI of human brain function during task activation. *Magn Reson Med* 25:390–397.
3. Kwong KK, et al. (1992) Dynamic magnetic resonance imaging of human brain activity during primary sensory stimulation. *Proc Natl Acad Sci USA* 89:5675–5679.
4. Biswal B, Yetkin FZ, Haughton VM, Hyde JS (1995) Functional connectivity in the motor cortex of resting human brain using echo-planar MRI. *Magn Reson Med* 34: 537–541.
5. Lowe MJ, Mock BJ, Sorenson JA (1998) Functional connectivity in single and multislice echoplanar imaging using resting-state fluctuations. *Neuroimage* 7:119–132.
6. Cordes D, et al. (2000) Mapping functionally related regions of brain with functional connectivity MR imaging. *AJNR Am J Neuroradiol* 21:1636–1644.
7. Greicius MD, Krasnow B, Reiss AL, Menon V (2003) Functional connectivity in the resting brain: A network analysis of the default mode hypothesis. *Proc Natl Acad Sci USA* 100:253–258.
8. Heeger DJ, Huk AC, Geisler WS, Albrecht DG (2000) Spikes versus BOLD: What does neuroimaging tell us about neuronal activity? *Nat Neurosci* 3:631–633.
9. Logothetis NK, Pauls J, Augath M, Trinath T, Oeltermann A (2001) Neurophysiological investigation of the basis of the fMRI signal. *Nature* 412:150–157.
10. Mukamel R, et al. (2005) Coupling between neuronal firing, field potentials, and FMRI in human auditory cortex. *Science* 309:951–954.
11. Leopold DA, Maier A (2012) Ongoing physiological processes in the cerebral cortex. *Neuroimage* 62:2190–2200.
12. Logothetis NK (2003) The underpinnings of the BOLD functional magnetic resonance imaging signal. *J Neurosci* 23:3963–3971.
13. Huttunen JK, Gröhn O, Penttonen M (2008) Coupling between simultaneously recorded BOLD response and neuronal activity in the rat somatosensory cortex. *Neuroimage* 39:775–785.
14. Schölvinck ML, Maier A, Ye FQ, Duyn JH, Leopold DA (2010) Neural basis of global resting-state fMRI activity. *Proc Natl Acad Sci USA* 107:10238–10243.
15. Magri C, Schridde U, Murayama Y, Panzeri S, Logothetis NK (2012) The amplitude and timing of the BOLD signal reflects the relationship between local field potential power at different frequencies. *J Neurosci* 32:1395–1407.
16. Engel SA, Glover GH, Wandell BA (1997) Retinotopic organization in human visual cortex and the spatial precision of functional MRI. *Cereb Cortex* 7:181–192.
17. Parkes LM, et al. (2005) Quantifying the spatial resolution of the gradient echo and spin echo BOLD response at 3 Tesla. *Magn Reson Med* 54:1465–1472.
18. Shmuel A, Yacoub E, Chaimow D, Logothetis NK, Ugurbil K (2007) Spatio-temporal point-spread function of fMRI signal in human gray matter at 7 Tesla. *Neuroimage* 35: 539–552.
19. Yacoub E, et al. (2001) Imaging brain function in humans at 7 Tesla. *Magn Reson Med* 45:588–594.
20. Uğurbil K, Toth L, Kim DS (2003) How accurate is magnetic resonance imaging of brain function? *Trends Neurosci* 26:108–114.
21. Kennan RP, Zhong J, Gore JC (1994) Intravascular susceptibility contrast mechanisms in tissues. *Magn Reson Med* 31:9–21.
22. Duong TQ, et al. (2003) Microvascular BOLD contribution at 4 and 7 T in the human brain: Gradient-echo and spin-echo fMRI with suppression of blood effects. *Magn Reson Med* 49:1019–1027.
23. Wang Z, et al. (2013) The relationship of anatomical and functional connectivity to resting-state connectivity in primate somatosensory cortex. *Neuron* 78:1116–1126.
24. Sheth SA, et al. (2004) Columnar specificity of microvascular oxygenation and volume responses: Implications for functional brain mapping. *J Neurosci* 24:634–641.
25. Kim DS, et al. (2004) Spatial relationship between neuronal activity and BOLD functional MRI. *Neuroimage* 21:876–885.
26. Powell TP, Mountcastle VB (1959) Some aspects of the functional organization of the cortex of the postcentral gyrus of the monkey: A correlation of findings obtained in a single unit analysis with cytoarchitecture. *Bull Johns Hopkins Hosp* 105:133–162.
27. Burton H, Sinclair RJ (1996) Somatosensory cortex and tactile perceptions. *Pain and Touch*, ed Kruger L (Academic Press, San Diego), 1st Ed, pp 105–177.
28. Reed JL, et al. (2008) Widespread spatial integration in primary somatosensory cortex. *Proc Natl Acad Sci USA* 105:10233–10237.
29. Wilson GH, 3rd, Yang PF, Gore JC, Chen LM (2016) Correlated inter-regional variations in low frequency local field potentials and resting state BOLD signals within S1 cortex of monkeys. *Hum Brain Mapp* 37:2755–2766.
30. Zhang N, Gore JC, Chen LM, Avison MJ (2007) Dependence of BOLD signal change on tactile stimulus intensity in SI of primates. *Magn Reson Imaging* 25:784–794.
31. Friedman RM, Chen LM, Roe AW (2008) Responses of areas 3b and 1 in anesthetized squirrel monkeys to single- and dual-site stimulation of the digits. *J Neurophysiol* 100: 3185–3196.
32. Chen L, et al. (2011) Fine-scale functional connectivity in somatosensory cortex revealed by high-resolution fMRI. *Magn Reson Imaging* 29:1330–1337.
33. Shi Z, et al. (2016) Realistic models of apparent dynamic changes in resting-state connectivity in somatosensory cortex. *Hum Brain Mapp* 37:3897–3910.
34. National Research Council (2011) *Guide for the Care and Use of Laboratory Animals* (National Academies Press, Washington, DC), 8th Ed.
35. Glover GH, Li TQ, Ress D (2000) Image-based method for retrospective correction of physiological motion effects in fMRI: RETROICOR. *Magn Reson Med* 44:162–167.
36. Snyder AZ (1992) Steady-state vibration evoked potentials: Descriptions of technique and characterization of responses. *Electroencephalogr Clin Neurophysiol* 84:257–268.